



Sharif University of Technology

Scientia Iranica

Transactions D: Computer Science & Engineering and Electrical Engineering

www.sciencedirect.com



Invited/Research note

Biopotential as predictor of ablation zone size during radiofrequency tumor ablation

D.J. Schutt^a, A.P. O'Rourke^b, J.A. Will^c, D. Haemmerich^{a,*}

^a Division of Pediatric Cardiology, Medical University of South Carolina, 165 Ashley Ave, MSC 915, Charleston, SC 29425, USA

^b Department of Surgery, University of Wisconsin-Madison, Clinical Science Center, P.O. Box 7375, 600 Highland Ave, Madison, WI 53792, USA

^c Department of Animal Health and Biomedical Sciences, University of Wisconsin-Madison, Animal Health & Biomedical Sciences Bldg, 1656 Linden Dr, Madison, WI 53706, USA

Received 26 October 2010; revised 7 December 2010; accepted 4 January 2011

KEYWORDS

Radiofrequency ablation;
RF ablation;
Thermal therapy;
Cancer;
Tumor ablation.

Abstract Biopotential is an electrochemical potential that has been shown to correlate well with the coagulation zone size during cardiac RF catheter ablation. We designed an in vivo experiment to test the hypothesis that a similar correlation exists during hepatic RF ablation. We created coagulation zones, in vivo, in porcine liver, with 17 gauge needle electrodes, using RF ablation ($n = 56$). The power was set constant at 30 W, controlled by impedance, and applied for 60, 120 or 180 s. We measured the biopotential between the electrode and the ground pad with low-pass filtering. The diameter and volume of the coagulation zone were measured and correlated with the change in biopotential between the beginning and end of each ablation procedure. Moderate correlation between biopotential change and both coagulation zone volume ($R^2 = 0.43$) and diameter ($R^2 = 0.31$) was observed. The time constant of the biopotential change was not significantly different from the time constant of the ablation zone diameter (36.6 s, $p = 0.93$); the biopotential may, therefore, predict the time course of the ablation zone diameter. The biopotential can potentially be used for intra-procedural monitoring of the progression of the thermal damage zone. It may also allow termination of the procedure, if it can be confirmed that the biopotential reliably correlates with the cessation of ablation zone expansion.

© 2011 Sharif University of Technology. Production and hosting by Elsevier B.V. All rights reserved.

1. Introduction

Primary liver cancer remains one of the most widespread cancers worldwide, with approximately 500,000 new cases per year [1]. Additionally, colorectal cancer is one of the most commonly diagnosed malignancies in the United States, with an estimated 150,000 new cases and 57,000 deaths annually [2]. A significant number of these deaths are as a result of metastatic liver tumors, which occur in nearly half of all colorectal cancer

cases [3]. The standard curative treatment for both types of hepatic cancer is surgical resection, with 5 year survival rates of 25%–50% [3–6]. However, only 10%–20% of cases are amenable to resection. This may be due to anatomic considerations (such as bilobar disease or proximity to vasculature), limited hepatic reserve or co-morbid disease creating high surgical risk [6,7].

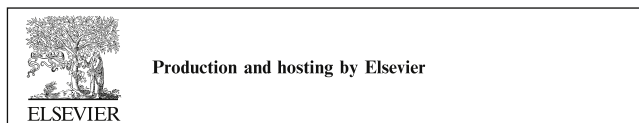
Over the past ten years, a number of technologies have emerged in the treatment of unresectable liver cancer, including cryoablation, microwave ablation, laser ablation and radiofrequency (RF) ablation [8]. Currently, RF ablation is the ablative modality used most widely, worldwide. In RF ablation, an electrode (typically 14–17 gauge) is first inserted into a liver tumor percutaneously, laparoscopically or during open surgery. Alternating electric current in the radiofrequency spectrum (typically 450–500 kHz) is then applied to the electrode, resulting in resistive heating of the tissue around the electrode. Over the course of a typical procedure, a roughly spherical area of tissue between 3 and 6 cm in diameter – depending on electrode type – is heated above 50 °C, resulting in coagulation necrosis. In addition to the management of hepatic cancer, RF ablation is increasingly being used to treat tumors in other soft organ tissue, including kidney, breast and lung, as well as bone marrow [9,10].

* Corresponding author.

E-mail address: haemmer@musc.edu (D. Haemmerich).

1026-3098 © 2011 Sharif University of Technology. Production and hosting by Elsevier B.V. All rights reserved. Peer review under responsibility of Sharif University of Technology.

doi:10.1016/j.scient.2011.08.018



Currently, a major limitation of RF ablation is the difficulty in determining the extent of thermal tissue damage during the course of each procedure. The primary real-time imaging modality used during RF procedures is intraoperative ultrasound (IOUS). During the monitoring of RF ablations with IOUS, a hyperechoic region forms in the area around the electrode, due to microbubbles generated during tissue boiling [11]. However, prior studies have demonstrated that this hyperechoic region does not accurately demarcate the zone of thermal coagulation [12]. This inability to accurately monitor the progress of the ablation in real-time reduces the efficacy of the treatment, lengthens procedural time, and necessitates lengthy (and often inconclusive) follow-up imaging [13]. Computerized tomography (or CT) can be used to accurately monitor the ablation zone during percutaneous RF ablation (the CT equipment is too constraining to be used during open surgical procedures). However, the time necessary for this imaging modality precludes it from practical use as a real time monitor of ablation zone formation.

Previous studies have demonstrated that a DC (direct current) electrochemical potential (hereafter, 'biopotential') develops between the active electrode and a reference electrode during cardiac catheter RF ablation of myocardial tissue [14,15]. It has been hypothesized that this biopotential is a result of free radicals and electrolytes released during tissue injury [14]. The magnitude of this biopotential correlated strongly with final ablation zone volume in prior studies [14,15]. We hypothesized that a measurable biopotential would similarly develop during RF ablation of liver tissue, and possibly allow real-time estimation of ablation zone dimensions.

2. Materials and methods

2.1. RF generator

We used a commercially available Valleylab 200 W Cool Tip generator and a Valleylab 17 gauge Cool Tip needle electrode to create all ablation zones. The stainless steel electrode had an exposed tip length of 3 cm. Cooling water was not circulated through the electrodes during the experiments, because it interfered with the formation of the biopotential signal in preliminary trials. Possibly, the region of sub-lethal temperatures surrounding the cooled ablation electrode hindered development of the potential. RF energy (460 kHz) was applied in a unipolar mode between the needle electrode and a large tin defibrillation dispersive electrode in contact with the animal's skin. The generator was operated, using an impedance controlled algorithm, in which a constant power is applied to the tissue until the measured impedance increases a predetermined amount over the baseline impedance (due to tissue vaporization near the electrode) [16]. At this point, the generator stops delivering energy for 15 s to allow the impedance to decline before reapplying power.

2.2. Biopotential

The biopotential signals developed during ablation were measured and recorded using a digital oscilloscope (Agilent 54621A) with 10 : 1 probes. We used a passive low-pass RC filter with a corner frequency of 7 Hz to isolate the biopotential signal from the applied RF power signal. Figure 1 is the schematic of the measurement circuit.

The value of the biopotential was determined by subtracting the starting potential from the lowest potential reached during each trial, as shown below in Figure 2. Note that the starting

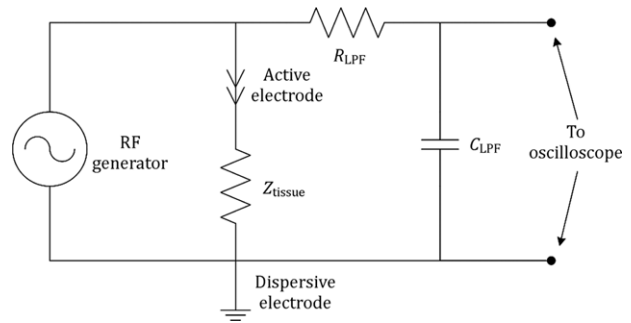


Figure 1: A low pass filter ($R_{LPF} = 976 \text{ k}\Omega$ and $C_{LPF} = 22 \text{ nF}$) between the electrodes and the oscilloscope removes the high frequency RF signal from the biopotential.

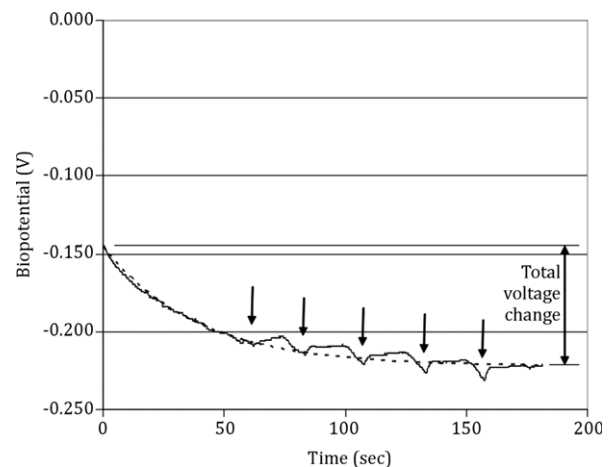


Figure 2: Biopotential waveform from a typical in vivo trial. The maximum voltage differential for each trial was used for correlation with ablation zone dimensions. The discontinuities (arrows) result from RF power being turned on/off, due to the impedance control algorithm used for power control. The dashed line represents the exponential approximation of this waveform [$v(t) = A \exp(-t/\tau) - (A - v(0))$]. For this particular trial, the values of A and τ were 0.077 and 38.3 s, respectively.

potential is larger than any cell membrane potential and is therefore not likely due to living tissue. Rather, it is likely due to the offset potential that develops when electrodes of dissimilar metals are placed into an electrolytic solution [17].

2.3. Animals

Pre-approval for all animal experiments was obtained from the Institutional Animal Care and Use Committee, University of Wisconsin, Madison. Six domestic swine (approximately 15–35 kg) were used in this study. The animals were first injected intramuscularly with a narcotic preanesthetic, Telazol®, then anesthetized with inhaled halothane and intubated via a tracheostomy. The abdominal wall was then incised to access the liver. At the conclusion of each experiment, the animals were euthanized by intracardial injection of potassium chloride.

2.4. Procedure

To create each ablation, the needle electrode was inserted into the liver at a suitable location, so that the entire exposed portion of the electrode was inside the tissue. 30 W of power

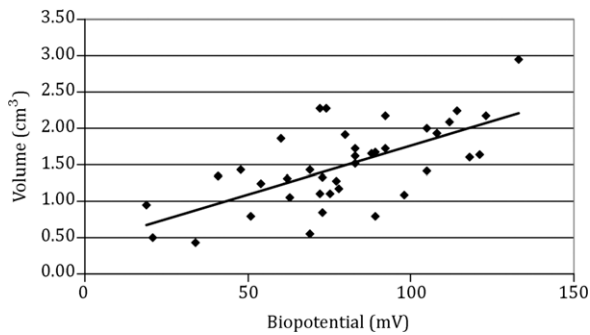


Figure 3: We observed a moderate correlation between the postfixation ablation zone volume and the magnitude of the biopotential signal ($R^2 = 0.43$).

were then applied to the electrode for 60, 120 or 180 s; the time of energy delivery was randomized to create ablation zones of different sizes. The biopotential signals observed during each ablation were recorded and saved for later analysis. After the required number of ablations was created, the animal was sacrificed and the ablated lobes of liver resected. The liver was then placed in 10% formalin for fixation.

2.5. Measurements

The fixed liver tissue was sliced perpendicularly to the direction of the electrode insertion and images of the slices taken with a digital camera. The software ImageJ (<http://rsb.info.nih.gov/ij/>) was used to measure the area, perimeter and diameter of the resulting ablation zones. Boundaries of tissue necrosis were determined by visual inspection. Ablation zone volume was calculated by multiplying the ablation zone area by the slice thickness, and summing for all slices. The diameter was measured as the value of the minor axis of the fitted ellipse for each slice of the ablation zone. Slices, where the ablation zone extended to the surface of the lobe, were excluded from the diameter measurement because of their nonsymmetry. The minor axis was chosen to account for any nonorthogonality in the tissue slicing. The diameter reported in the results below is the maximum value of all the slices for each ablation zone. Pearson's correlation coefficient (R^2) was used to analyze correlations between ablation zone dimensions and the biopotential for each trial.

We fit an exponential function by minimizing the square of error to the relationship between the ablation zone volume (V) versus time, and the diameter (d) versus time: e.g. $d(t) = A(1 - \exp(-t/\tau))$, with amplitude A and time constant τ . Similarly, we fitted an exponential function to each of the biopotential time courses (see Figure 2). We used the Student's t -test to determine whether there is a difference between the time constants of ablation zone growth (volume and diameter) and biopotential change.

3. Results

A total of 56 RF ablations were performed and analyzed in this study. Figure 3 shows the moderate correlation ($R^2 = 0.43$) between the biopotential change and the corresponding ablation zone volume.

Figure 4 shows the relationship between maximum ablation zone diameter and the biopotential. The correlation between this parameter and the biopotential change was not as strong ($R^2 = 0.31$).

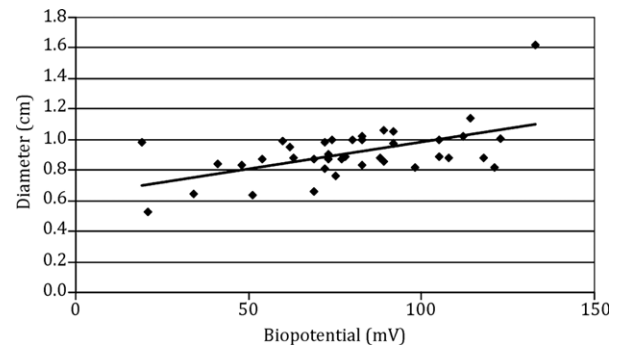


Figure 4: Correlation between the postfixation maximum ablation zone diameter and the magnitude of the biopotential signal was weaker than that for the volume ($R^2 = 0.31$).

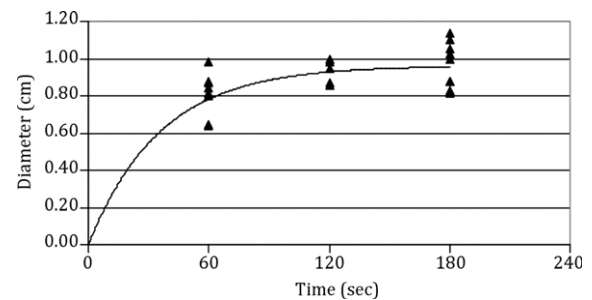


Figure 5: The diameter data were fitted to an exponential curve of the form $f(t) = A(1 - \exp(-t/\tau))$. The values of A and τ were 0.962 and 35.8 s, respectively.

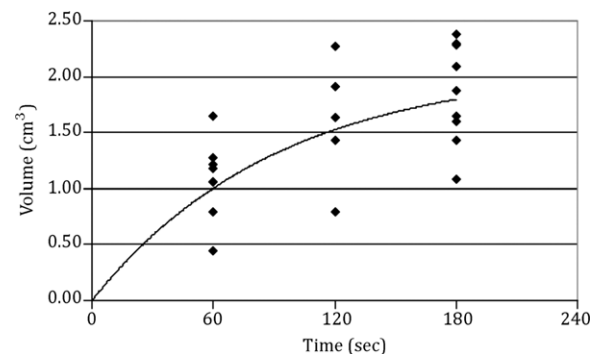


Figure 6: The volume data were fitted to an exponential curve of the form $f(t) = A(1 - \exp(-t/\tau))$. The values of A and τ were 2.09 and 91.7 s, respectively.

While we expect some difference in correlation between the biopotential and either the diameter or volume, from our data, it is unclear which of these two parameters shows the better correlation.

The time constants for ablation zone volume (V) and diameter (d) were 91.7 s and 35.8 s, respectively (see Figures 5 and 6). The time constant for biopotential change was 36.6 ± 37.7 s, and was significantly different from the time constant for ablation zone volume ($p < 0.001$), but not the diameter ($p = 0.93$).

During several of the trials ($n = 26$), there were rapid voltage changes or "spikes" in the biopotential waveform. Figure 7 shows an example of this phenomenon.

These trials were not included in the results, because we believed the voltage spikes caused the magnitude of the measured potential to be overstated.

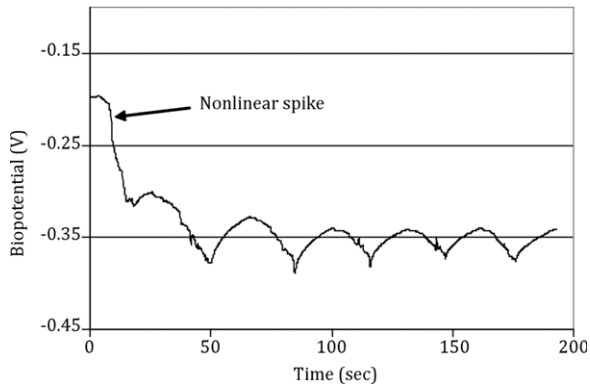


Figure 7: An example of the nonlinear “spike” in magnitude of the biopotential signal recorded during some of the trials.

4. Discussion

Currently, a significant limitation of RF ablation is the inability to accurately image the ablation zone during treatment. While IOUS is the current standard for imaging open RF ablations, it tends to overestimate the size of the ablation zone. We postulated that biopotential changes could help predict the size and growth of the ablation zone more accurately. We demonstrate that biopotential increased in all cases during the course of treatment. We further demonstrate that increasing biopotential was associated with an increase in ablation zone dimensions. From a clinical standpoint, however, the correlation is not strong enough to suggest clinical use at this point. Though the biopotential signal was not helpful in assessing the size of the ablation zone, it may assist in determining the duration of treatment. During longer trials, i.e. 3 min, the magnitude of the signal stopped increasing near the end of the ablation (see Figure 2). This could allow us to determine when the ablation zone stops increasing in size, indicating that the ablation procedure can be terminated, since the continued application of RF energy will not result in further growth of the ablation zone.

Currently, constant ablation time is typically used for each procedure (12–45 min, depending on device); e.g. for the Valleylab Cool-tip ablation system, the procedural time of 12 min is based on a study performed by Goldberg et al. [18]. However, electrical and thermal tissue properties (especially blood perfusion) differ from organ to organ, from healthy to tumor tissue, and even from location to location within each organ. Therefore, since the thermodynamic conditions are different at each ablation site, the required application time is also likely different for each procedure. By monitoring the biopotential, we may be able to determine when each ablation zone has reached its maximum size and terminate the procedure, thus using optimal treatment time. To investigate this possibility, we compared the time constants of ablation zone growth and biopotential change. While the time constant of the ablation zone volume was much longer (92 s, $p < 0.001$), the ablation zone diameter had a time constant (35.8 s) close to that of the biopotential (36.6 s, $p = 0.93$). However, since we do not have data on ablation zone growth for each trial, but only an estimate based on cumulative data from all trials, further experiments are necessary, which acquire data on ablation zone growth versus time during each trial (either by imaging or multiple temperature measurements).

4.1. Limitations

As mentioned above, previous studies have shown a strong correlation between the magnitude of the biopotential observed during the cardiac catheter RF ablation of the myocardium and ablation zone dimensions [14,15]. In the present study, analysis of the relationship between the biopotential and final ablation zone dimensions, using porcine liver tissue, was less conclusive. There were several differences in our experimental methodology that may account for the weaker observed correlation. The RF generator used in our study did not automatically ramp up the power applied to the tissue at the beginning of each trial; the power was manually adjusted to a final value of 30 W over a period of approximately 5 s. Irregularities in this adjustment may have caused some or all of the waveform “spikes” noted in the previous section (Figure 7), again possibly as a result of polarization of the electrodes during the initial application of RF energy. Any nonlinear effects may have been more pronounced in this study, due to the difference in materials between cardiac electrodes (platinum) and those used in this study (stainless steel). Additionally, our measurements of ablation zone volume and diameter may have been less accurate due to the small volume of coagulated tissue formed during ablations using a single needle electrode (without cooling). Additional experiments, where ablation zones of similar size as clinically seen (3–6 cm diameter) are required to further determine the utility of the biopotential in monitoring ablation zone formation.

5. Conclusion

One current shortcoming of tumor radiofrequency ablation procedures is insufficient intraprocedural information about ablation zone size. The biopotential investigated in this study may provide this missing information. Furthermore, it may allow the termination of radiofrequency ablation procedures when the ablation zone has reached its maximum size, possibly reducing currently lengthy treatment times.

Acknowledgments

This work was supported by the National Institute of Health, Grant DK058839, and Grant C06 RR018823 from the Extramural Research Facilities Program of the National Center for Research Resources.

References

- [1] Bosch, F.X., Ribes, J., Cléries, R. and Diaz, M. “Epidemiology of hepatocellular carcinoma”, *Clin. Liver Dis.*, 9(2), pp. 191–211 (2005).
- [2] Jemal, A., Tiwari, R.C., Murray, T., Ghafoor, A., Samuels, A., Ward, E., Feuer, E.J. and Thun, M.J. “Cancer statistics 2010”, *CA Cancer J. Clin.*, 60(5), pp. 277–300 (2010).
- [3] Yoon, S.S. and Tanabe, K.K. “Surgical treatment and other regional treatments for colorectal cancer liver metastases”, *Oncologist*, 4, pp. 197–208 (1999).
- [4] Fong, Y., Fortner, J., Sun, R.L., Brennan, M.F. and Blumgart, L.H. “Clinical score for predicting recurrence after hepatic resection for metastatic colorectal cancer: analysis of 1001 consecutive cases”, *Ann. Surg.*, 230(3), pp. 309–321 (1999).
- [5] Usatoff, V. and Habib, N. “Hepatic malignancy: challenges and opportunities for the surgeon”, *J. R. Coll. Surg. Edinb. UK*, 45(2), pp. 99–109 (2000).
- [6] Poon, R.T.P., Fan, S.T., Tsang, F.H.F. and Wong, J. “Locoregional therapies for hepatocellular carcinoma: a critical review from the surgeon’s perspective”, *Ann. Surg.*, 235(4), pp. 466–486 (2002).
- [7] Cha, C., Lee Jr., F.T., Rikkens, F.T., Niederhuber, J.E., Nguyen, B.T. and Mahvi, D.M. “Rationale for the combination of cryoablation with surgical resection of hepatic tumors”, *J. Gastrointestinal Surg.*, 5(2), pp. 206–213 (2001).

- [8] Dodd III, G.D., Soulen, M.C., Kane, R.A., Livraghi, T., Lees, W.R., Yamashita, Y., Gillams, A.R., Karahan, O.I. and Rhim, H. "Minimally invasive treatment of malignant hepatic tumors: at the threshold of a major breakthrough", *Radiographics*, 20, pp. 9-27 (2000).
- [9] Simon, C.J., Dupuy, D.E., DiPetrillo, T.A., Safran, H.P., Grieco, C.A., Ng, T. and Mayo-Smith, W.W. "Pulmonary radiofrequency ablation: long-term safety and efficacy in 153 patients", *Radiology*, 243, pp. 268-275 (2007).
- [10] Gillams, A. "Tumour ablation: current role in the liver, kidney, lung and bone", *Cancer Imag.*, 8(S1-5), (2008).
- [11] Goldberg, S.N. and Dupuy, D.E. "Image-guided radiofrequency tumor ablation: challenges and opportunities – part I", *J. Vasc. Interv. Radiol.*, 12(9), pp. 1021-1032 (2001).
- [12] Goldberg, S.N., Walovitch, R., Halpern, E.F. and Gazelle, G.S. "Immediate detection of radiofrequency induced coagulation necrosis using a novel ultrasound contrast agent", *Radiology*, 213, pp. 438-444 (1999).
- [13] Hsu, C.P., Razavi, M.K., So, S.K., Parachikov, I.H. and Benaron, D.A. "Liver tumor gross margin identification and ablation monitoring during liver radiofrequency treatment", *J. Vasc. Interv. Radiol.*, 16(11), pp. 1473-1478 (2005).
- [14] Erdogan, A., Carlsson, J., Grumbrecht, S., Kostin, S., Schulte, B., Schlapp, M., Neuzner, J. and Pitschner, H.F. "Electrochemical potentials during radiofrequency energy delivery: a new method to control catheter ablation of arrhythmias", *Europace*, 3, pp. 201-207 (2001).
- [15] He, D.S., Sharma, P., Wang, X., Bosnos, M. and Marcus, F. "Bio-battery signal predicts myocardial lesion formation and depth in vitro", *J. Interv. Card. Electrophysiol.*, 3, pp. 69-77 (1999).
- [16] McGahan, J.P. and Dodd, G.D. "Radiofrequency ablation of the liver: current status", *Am. J. Roentgenol.*, 176, pp. 3-16 (2001).
- [17] Neuman, M.R. "Biopotential electrodes", In *Instrumentation: Application and Design*, J.G. Webster, Ed., 3rd Edn., pp. 183-185, John Wiley & Sons, Inc., New York (1998).
- [18] Goldberg, S.N., Stein, M.C., Gazelle, G.S., Sheiman, R.G., Kruskal, J.B. and Clouse, M.E. "Percutaneous radiofrequency tissue ablation: optimization of pulsed radiofrequency technique to increase coagulation necrosis", *J. Vasc. Interv. Radiol.*, 10, pp. 907-916 (1999).

David J. Schutt was born in Wyandotte, MI, in 1977. He received a B.S. degree from the Department of Electrical Engineering at the University of Wisconsin, Madison in 2000, and an M.S. degree from the Department of Biomedical Engineering at the same university, in 2005. He is currently a Research Specialist in the Division of Pediatric Cardiology at the Medical University of South Carolina, Charleston. His research interests include tumor ablation, cardiac ablation and biomedical instrumentation.

Ann P. O'Rourke received a B.S. degree from Emory University, Atlanta, GA, in 1993 and M.D. and M.S. degrees in Public Health from the University of Wisconsin-Madison in 2002 and 2006, respectively.

She is a Resident in General Surgery and a Surgical Oncology Research Fellow at the University of Wisconsin Hospital.

James A. Will received B.S. and M.S. degrees from the University of Wisconsin-Madison in 1952 and 1953, respectively, and the DVM from Kansas State University, Manhattan, KS, in 1960. After private practice, he returned to the University of Wisconsin-Madison and obtained a Ph.D. degree in 1967. He is Professor Emeritus of Veterinary Medicine, SVM, Surgery, Medical School, Biomedical Engineering, COE and Animal Science, CALS, at the University of Wisconsin-Madison. He teaches cardiovascular and renal physiology to undergraduate and graduate students and is involved with the biological training of graduate students in biomedical engineering. He is currently doing experimental surgery research in the development of devices for hepatic tumor ablation.

Dieter Haemmerich received his Ph.D., BME degree from the University of Wisconsin-Madison in 2001, and his Ph.D., E.E. degree from the Vienna University of Technology in 2003. He is currently Associate Professor of Pediatric Cardiology at the Medical University of South Carolina, and Adjunct Faculty of Bioengineering at Clemson University. His research interests include thermal ablation, biomedical instrumentation, measurement of thermal and dielectric tissue properties, and computational modeling of biological heat transfer problems and targeted drug delivery (see ablation.musc.edu).